Kathmandu University
Journal of Science, Engineering and Technology

Differential transform method approach to the study of an MHD flow of a third grade fluid with Reynolds' model viscosity and Joule heating

M. O. Iyoko* and B. I. Olajuwon

Department of Mathematics, Federal University of Agriculture Abeokuta, Ogun State, Nigeria.

Abstract

For this research, the Differential Transform Method (DTM) approach was considered in studying a fluid of third grade; which is non-Newtonian, inside a circular duct experiencing a magnetic force and joule heating. We considered Reynolds' model viscosity in the analysis. In the situation where the joule heating parameter (J) together with the magnetic parameter (M) are zero ($J = M = 0$), results of the mid-point (where $r = 0$) temperature ($\theta(0)$) shows that the Differential Transform Method's convergence as compared to the Adomian decomposition method (ADM) solution is faster. The difference between Differential Transform Method and the Adomian solution is about 10^{-2}. The results of the fluid's velocity as well as temperature are presented as graphs, from which we found out that: increment of magnetic force reduces both velocity and temperature of the fluid and higher values of joule heating factor causes velocity of the flow to increase, while increment in joule heating factor reduces the fluid's temperature midpoint of the duct.

Keywords: Differential transform method; Third grade fluid; Magnetohydrodynamics; Joule heating; Reynolds' model viscosity

1. Introduction

The Fourier and Laplace transform methods are used to solve various problems in engineering. They create algebraic equations from differential equations for ease in solution of such problems. But, when applying to nonlinear problems, these methods become sophisticated and tough to handle. One method through which this difficulty can be surmounted is the Differential Transform Method (DTM). The DTM was used by [1] for solving a circuit problem in engineering. As a derivation from Taylor series expansion, the DTM creates a polynomial as analytic results. For the DTM approach, there is no need to compute the individual derivatives of the functions as it is done in the Taylor series method.

Differential transform posses the intrinsic competence to handle nonlinear mathematical challenges. Also, it is applied in solving ODE's as well as PDE's. The DTM in two-dimension was used by [2] to solve PDE's. Previous researchers such as [3-6] utilized the DTM approach to find answers to different problems. The convergence of the DTM was discussed by [7] and there was a presentation of various numerical examples. The use of DTM in solving the nonlinear D.E controlling Jeffery-Hamel flow, where a large magnetic field existed was done in the findings of [8]. Also, [9] applied the DTM to find solutions to parabolic PDE's of fourth-order.

Obtaining approximations which are analytic for non-linear PDE's has been arduous up to this present time, although there are computer softwares and computers whose performances are high. The regular and homotopy perturbation method was operational in [10] where they found a solution to the problem of the yield of heat transfer; as well as suction on the flow of a thin film of a third grade fluid via a sloped medium that was porous. A mathematical model was created by [11] to find the approximate value of a natural smoldering log's temperature, positions and burn rate. A unique class of Hermite-Pade approximants based scheme was used by [12] for solving the problem of an optically thin fluid flow, with variable viscosity via a conduit with isothermal walls. [13] studied a fluid of third grade that is reactive with a viscosity model of the Reynold's type in a flat channel and the elimination of criticality for such fluid.

Magnetohydrodynamics (MHD), as initially presented by Alfvén in 1970 [14], has to do with causing the formation of current inside a fluid in motion that is conductive and surrounded by a magnetic field; this induced current causes a force to act on the fluids' ions. James Prescott Joule's research in 1841 followed by Heinrich Lenz's work of 1842 brought about the discovery of Joule heating--this phenomenon involves the discharge of heat from a conductor when a current of electricity is passed through it. The square of the electric current is in proportion to the quantity of the heat discharged from the conductor. Magnetohydrodynamics (MHD) has been applied when making the blueprint of cooling networks that has flowing metals. Also, the making of various flow meters, MHD generators, pumps and accelerators rely on the use of Magnetohydrodynamics [15-18]. These and many other applications made MHD channels very interesting to researchers; hence, they began to study it. For example, where the magnetic field of the earth begins and -weather prediction can be interpreted with the help of MHD. Also, MHD can explain why turbulent shifts of molten semiconductors become damped whenever crystals are growing, and it can be used in food production companies to determine the rate at which beverages flow [19-21]. The joint influences of slip boundary and Joule heating on the Magnetohydrodynamics third grade fluid that flow downward of a plane which is tilted, was the center of consideration in [22,23].

Third grade fluids are materials displaying qualities of both ideal

*Corresponding author. Email: mikiyoks@gmail.com

fluids and elastic solids and unveiling partial elastic recovery; after deformation. Third grade fluids are classified as 'visco-elastic fluids', and they are of great importance when it comes to problems involving heat transfer. They have various applications in science, industry and technology. Hence, many researchers in recent times have been paying attention to their study. A heat generation and viscous dissipation model in single dimension for a fluid of third grade, flowing inside a cylindrical duct was studied by [24] using the regular perturbation technique. It established an excellent agreement with the results from the finite difference method. [25] extended this work with the incorporation of Magnetohydrodynamics (MHD) together with Joule heating as part of the model, which was then solved for velocity and temperature, utilizing the Adomian decomposition method. They concluded that the fluid's velocity decreases while there is increase in temperature when magnetic parameter is varied. Also, the heat generation parameter's influence is turned around by the joule heating parameter.

Here therefore, we have discussed the DTM approach by which approximate solutions can be found for the velocity and temperature of the extended model. Considering the Reynolds' model viscosity, we compared the results of DTM to the Adomian decomposition method (ADM) solution. Maple 13 was utilized to execute the codes generated to determine results.

2. Materials and methods

2.1. Differential transform method essentials

Reckon that a domain A contains an analytical function $s(t)$, and $t = t_0$ describes any point inside A, where $s(t)$ is a power series with mid-point at t. The function $s(t)$ has its Taylor series expansion given as:

$$s(t) = \sum_{k=0}^{\infty} \frac{(t-t_0)^k}{k!} \left[\frac{d^k s(t)}{d\,t^k}\right]_{t=t_0} \quad \forall x \in A \tag{1}$$

When $t_0 = 0$, equation (1) is called a Maclaurin series for $s(t)$; defined by:

$$s(t) = \sum_{k=0}^{\infty} \frac{t^k}{k!} \left[\frac{d^k s(t)}{d\,t^k}\right]_{t=0} \quad \forall x \in A \tag{2}$$

The function $s(t)$ has its Differential transform outlined as:

$$S(k) = \sum_{k=0}^{\infty} \frac{1}{k!} \left[\frac{d^k s(t)}{d\,t^k}\right]_{t=0} \tag{3}$$

Here, the transformed function is $S(k)$ while original function is $s(t)$. An inverse differential transform is given by:

$$s(t) = \sum_{k=0}^{\infty} S(k)\, t^k \tag{4}$$

2.2. The third grade fluid flow model

The fluid is flowing steadily inside a cylindrical duct whose length is infinite. As depicted by Fig. 1 below.

[26] together with [27] gave the model equations which [28] did an extension by adding a source term. Adding effect of a magnetic field as well as joule heating to the model equations gives:

$$\frac{1}{\overline{r}}\frac{d}{d\overline{r}}\left(\overline{r}\,(2\alpha_1+\alpha_2)\left[\frac{d\overline{w}}{d\overline{r}}\right]^2\right) = \frac{\partial \overline{p}}{\partial \overline{r}} \tag{5}$$

$$0 = \frac{\partial \overline{p}}{\partial \overline{\phi}} \tag{6}$$

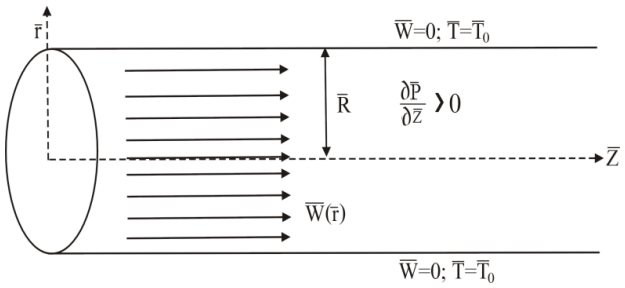

Figure 1: Flow model in cylindrical coordinate.

$$\frac{1}{\overline{r}}\frac{d}{d\overline{r}}\left(\overline{r}\,\overline{\mu}\frac{d\overline{w}}{d\overline{r}}\right) + \frac{1}{\overline{r}}\frac{d}{d\overline{r}}\left(2\overline{r}\beta_3\left[\frac{d\overline{w}}{d\overline{r}}\right]^3\right) - \sigma\beta_0^2\overline{w} = \frac{\partial \overline{p}}{\partial \overline{z}} \tag{7}$$

$$K\left(\frac{1}{\overline{r}}\frac{d}{d\overline{r}}\left(\overline{r}\frac{d\overline{T}}{d\overline{r}}\right)\right) + \overline{\mu}\left[\frac{d\overline{w}}{d\overline{r}}\right]^2 + 2\beta_3\left[\frac{d\overline{w}}{d\overline{r}}\right]^4 + \overline{QC}_0\left(\overline{T}-\overline{T}_0\right) + \sigma\beta_0^2\overline{w}^2 = 0 \tag{8}$$

The boundary conditions needed to get a solution to (7) and (8) are given as

$$\overline{w}(\overline{R}) = \overline{T}(\overline{R}) = 0,\ \frac{d\overline{w}}{d\overline{r}}(0) = \frac{d\overline{T}}{d\overline{r}}(0) = 0 \tag{9}$$

The definition of the model parameters are found in Table 2 below. When $\overline{Q} > 0$, there is heat generation, whereas $\overline{Q} < 0$ means heat absorption. Magnetic effect is represented by $\sigma\beta_0^2\overline{w}$, while $\sigma\beta_0^2\overline{w}^2$ refers to the joule heating term. To get any $\frac{\partial \overline{p}}{\partial \overline{z}}$, integration of (7) is carried out and after determining the flow field, equation (5) and (7) are used to derive the actual pressure field. The momentum equation is represented by (7) whereas the energy equation is given by (8).

Using the similarity transformations:
$r = \frac{\overline{r}}{\overline{R}}$, $w = \frac{\overline{w}}{\overline{w}_0}$, $\mu = \frac{\overline{\mu}}{\overline{\mu}_0}$ the non-dimensional equations relating to (7), (8) and (9) respectively are as follows:

$$\frac{d\mu}{dr}\frac{dw}{dr} + \frac{\mu}{r}\left(\frac{dw}{dr} + r\frac{d^2w}{dr^2}\right) + \frac{\Lambda}{r}\left[\frac{dw}{dr}\right]^2\left(\frac{dw}{dr} + 3r\frac{d^2w}{dr^2}\right) - Hw = C \tag{10}$$

$$\frac{d^2\theta}{dr^2} + \frac{1}{r}\frac{d\theta}{dr} + \Gamma\left(\frac{dw}{dr}\right)^2\left(\mu + \Lambda\left(\frac{dw}{dr}\right)^2\right) + \delta\theta + Jw^2 = 0 \tag{11}$$

with boundary conditions

$$w(1) = \theta(1) = 0,\ \frac{dw}{dr}(0) = \frac{d\theta}{dr}(0) = 0 \tag{12}$$

The viscosity model determines the way (10) and (11) looks like, and μ which is the viscosity is a temperature function by assumption. In this paper we shall use the Reynold's model viscosity case which is given by [29] and other works as:

$$\overline{\mu}(\overline{T}) = \overline{\mu}_0 \exp(-M(\overline{T}-\overline{T}_0)) \tag{13}$$

The fact that increment of temperature reduces Reynolds viscosity for liquids anytime there is a positive value for M, is undisputed. Also, in the case of gases increasing temperature bring about increase in Reynolds viscosity any time there is a negative value for M. A large value for M, means we can disregard the influence of

Table 1: Some basic Differential Transform Method operations.

Original function	Transformed function
$s(t) = au(t) \pm bv(t)$	$S(k) = aU(k) \pm bV(k)$
$s(t) = u'(t)$	$S(k) = (k+1)U(k+1)$
$s(t) = u''(t)$	$S(k) = (k+1)(k+2)U(k+2)$
$s(t) = u^n(t)$	$S(k) = (k+1)(k+2)(k+3)\cdots(k+n)U(k+n)$
$s(t) = u(t)v(t)$	$S(k) = \sum_{l=0}^{k} U(l)V(k-l)$
$s(t) = u(t)v(t)w(t)$	$S(k) = \sum_{l=0}^{k}\sum_{m=0}^{k-l} U(l)V(m)W(k-l-m)$
$s(t) = \alpha t^m$	$S(k) = \alpha\delta(k-m) = \begin{cases} 1, & k = m \\ 0, & k \neq m \end{cases}$
$s(t) = e^{\eta t}$	$S(k) = \frac{\eta^k}{k!}$
$s(t) = (1+t)^n$	$S(k) = \frac{n(n-1)(n-2)\cdots(n-k+1)}{k!} = {}^nC_k$
$s(t) = u^n(t)v^m(t)$	$S(k) = \sum_{l=0}^{k}\left(\prod_{i=1}^{n}(l+i)\right)\left(\prod_{i=1}^{m}(k-l+i)\right)U(l+n)V(k-l+m)$
$s(t) = u^n(t)v^m(t)w^p(t)$	$S(k) = \sum_{q=0}^{k}\sum_{r=0}^{k-q}\left(\prod_{i=1}^{n}(q+i)\right)\left(\prod_{j=1}^{m}(r+j)\right)\left(\prod_{l=1}^{p}(k-q-r+l)\right)U(r+n)V(k-r+m)W(k-q-r+p)$
$s(t) = u(t)v^n(t)w^m(t)$	$S(k) = \sum_{q=0}^{k}\sum_{r=0}^{k-q}\left[\left(\prod_{i=1}^{n}(q+i)\right)\left(\prod_{j=1}^{m}(r+j)\right)U(k)V(r+n)W(k-r+m)\right]$
$s(t) = u(t)v^n(t)w^m(t)x^p(t)$	$S(k) = \sum_{q=0}^{k}\sum_{r=0}^{k-q}\sum_{t=0}^{k-q-r}\left[\begin{array}{l}\left(\prod_{i=1}^{n}(q+i)\right)\left(\prod_{j=1}^{m}(k-r+j)\right)\left(\prod_{l=1}^{p}(k-q-r+l)\right) \\ U(k)V(k-r+n)W(k-q-r+m)X(k-q-r-t+p)\end{array}\right]$
$s(t) = u^n(t)v^m(t)w^p(t)x^v(t)$	$S(k) = \sum_{q=0}^{k}\sum_{r=0}^{k-q}\sum_{t=0}^{k-q-r}\left[\begin{array}{l}\left(\prod_{i=1}^{n}(q+i)\right)\left(\prod_{j=1}^{m}(k-r+j)\right)\left(\prod_{l=1}^{p}(k-q-r+l)\right) \\ \left(\prod_{w=1}^{v}(k-q-r-t+w)\right)U(r+n)V(k-r+m)W(k-q-r+p) \\ X(k-q-r-t+v)\end{array}\right]$

variable viscosity. Carrying out dimensional analysis for equation (13) we get:

$$\mu = \exp(-\rho\theta) \tag{14}$$

where ρ is the Reynold's viscosity variational parameter. Applying the Maclaurin's series to equation (14) gives:

$$\mu = 1 - \rho\theta + \mathrm{O}(\rho^2) \tag{15}$$

This implies that

$$\mu^{-1} = 1 + \rho\theta + \mathrm{O}(\rho^2) \tag{16}$$

2.3. The Differential Transform Method (DTM) approach to model

We can write equation (10) as

$$\frac{d^2w}{dr^2} + \frac{1}{r}\frac{dw}{dr} + \mu^{-1}\frac{d\mu}{dr}\frac{dw}{dr} + \frac{\Lambda}{r}\mu^{-1}\left[\frac{dw}{dr}\right]^3 + 3\Lambda\left[\frac{dw}{dr}\right]^2\frac{d^2w}{dr^2} - \mu^{-1}Hw = C\mu^{-1} \tag{17}$$

Neglecting $O(\rho^2)$ in (15) and (16), it implies that $\frac{d\mu}{dr} = -\rho\frac{d\theta}{dr}$ and

$$\mu^{-1} = 1 + \rho\theta \tag{18}$$

Substituting (18) in (17), expanding and collecting terms leads to

$$\frac{d^2w}{dr^2} = \frac{1}{\left(1 + 3\Lambda\left[\frac{dw}{dr}\right]^2\right)}\left[\rho\frac{dw}{dr}\frac{d\theta}{dr} + \rho^2\theta\frac{dw}{dr}\frac{d\theta}{dr} - \frac{1}{r}\frac{dw}{dr} - \frac{\Lambda}{r}\left[\frac{dw}{dr}\right]^3 - \frac{\rho\Lambda}{r}\theta\left[\frac{dw}{dr}\right]^3 + Hw + \rho H\theta w + C + \rho C\theta\right] \tag{19}$$

Applying the differential transforms as in Table 1 to (18) the differential transform of the momentum equation is

$$\begin{aligned} W(k+2) = {} & \frac{1}{(k+2)(k+1)\left[1 + 3\Lambda\sum_{r=0}^{k-s}(r+1)(k-r+1)W(r+1)W(k-r+1)\right]} \\ & \rho\sum_{r=0}^{k-s}(r+1)(k-r+1)W(r+1)\theta(k-r+1) + \rho^2\sum_{s=0}^{k}\sum_{r=0}^{k-s}(s+1)(r+1)\theta(k)W(r+1)\theta(k-r+1) \\ & -\tfrac{1}{r}(k+1)W(k+1) - \tfrac{\Lambda}{r}\sum_{s=0}^{k}\sum_{r=0}^{k-s}(s+1)(r+1)(k-r+1)W(r+1)W(k-r+1)W(k-s-r+1) - \\ & \tfrac{\rho\Lambda}{r}\sum_{s=0}^{k}\sum_{r=0}^{k-s}\sum_{t=0}^{k-s-r}(s+1)(r+1)(k-r+1)(k-s-r+1)\theta(k)W(k-r+1)W(k-s-r+1)W(k-s-r-t+1) + \\ & HW(k) + C\delta(k-m) + \rho H\sum_{r=0}^{k-s}\theta(m)W(k-m) - \rho C\theta(k) \end{aligned} \tag{20}$$

With boundary condition $W(1) = 0, W(0) = \lambda$, where we can use $W(1) = 0$, that is, $\sum_{k=0}^{n} W(k) = 0$ to get the function λ.

Substituting (15) in (11) and expanding gives the energy equation as

$$\frac{d^2\theta}{dr^2} = -\frac{1}{r}\frac{d\theta}{dr} - \Gamma\left[\frac{dw}{dr}\right]^2 + \rho\Gamma\theta\frac{dw}{dr}\frac{dw}{dr} - \Lambda\Gamma\left[\frac{dw}{dr}\right]^4 - \delta\theta - Jw^2 \tag{21}$$

Applying the differential transforms in Table 1 to (21), we get the differential transform of the energy equation as

$$\begin{aligned} \theta(k+2) = {} & \tfrac{1}{(k+2)(k+1)} \\ & \Bigg[-\tfrac{1}{r}(k+1)\theta(k+1) - \Gamma\sum_{r=0}^{k-s}(r+1)(k-r+1)W(r+1)W(k-r+1) + \rho\Gamma\sum_{s=0}^{k}\sum_{r=0}^{k-s}(s+1)(r+1)\theta(k)W(r+1)W(k-r+1) \\ & -\Lambda\Gamma\sum_{s=0}^{k}\sum_{r=0}^{k-s}\sum_{t=0}^{k-s-r}(s+1)(r+1)(k-r+1)(k-s-r+1)W(r+1)W(k-r+1)W(k-s-r+1)W(k-s-r-t+1) \\ & -\delta\theta(k) - J\sum_{m=0}^{k}W(m)W(k-m) \Bigg] \end{aligned} \tag{22}$$

$$W(1) = 0$$

$$W(2) = \frac{1}{2}H\lambda + \frac{1}{2}C + \frac{1}{2}\rho H\lambda^2 - \frac{1}{2}\rho C\lambda$$

$$W(3) = -\frac{2}{3r}\left(\frac{1}{2}H\lambda + \frac{1}{2}C + \frac{1}{2}\rho H\lambda^2 - \frac{1}{2}\rho C\lambda\right)$$

Table 2: Model parameters definition

	Dimensional perpendicular dist. from pipe axis	Greek symbols	
$\overline{r}$	Dimensionless perpendicular distance from pipe axis	α_1, α_2, and β_3	Constant material coefficients
$\overline{R}$	Radius of the pipe	$\beta = \frac{R\overline{T}_0}{E}$	Activation energy
$\overline{T}_0$	The initial temperature	$\rho = \overline{M}\beta\overline{T}_0$	Reynold's Viscosity Variational Parameter
$\overline{w}(\overline{R})$	Dimensional velocity component in the axis	$\overline{\mu}$	Dynamic shear viscosity
$w = \frac{\overline{w}}{\overline{w}_0}$	Dimensionless velocity component in the axis	$\mu = \frac{\overline{\mu}}{\overline{\mu}_0^e}$ or $\overline{\mu}_0^e = \{\overline{\mu}_0 = \mu_0 \exp(\overline{T}_0)\}$	Dimensionless viscosity
$\overline{w}_0$	Dimensional reference velocity	ϕ	Rotational direction
$\overline{z}$	Axis of the cylinder	$\theta = \frac{(\overline{T}-\overline{T}_0)E}{R\overline{T}_0^2}$	Dimensionless temperature excess
$C = \frac{\overline{R}^2}{\overline{w}_0\overline{\mu}_0}\frac{\partial\overline{p}}{\partial\overline{z}}$	Pressure gradient parameter	$\theta = \frac{4\overline{\mu}_0^e\overline{w}_0^2}{K\beta\overline{T}_0}$	Viscous heating parameter
K	Constant thermal conductivity	$\Lambda = \frac{\beta_3\overline{w}_0^2}{\overline{\mu}_0\overline{r}_0^2}$	Non-Newtonian material parameter of the fluid
$\frac{\partial\overline{p}}{\partial\overline{r}}$	Pressure gradient along the normal to the pipe axis	$\delta = \frac{\overline{Q}EA_0\overline{R}^2\overline{C}_0}{KR\overline{T}_0^2}$	Heat generation parameter
$\frac{\partial\overline{p}}{\partial\overline{z}}$	Pressure gradient in the axial direction	$H = \frac{\sigma\overline{R}^2\beta_0^2}{\mu_0}$	Magnetic Effect Parameter
$\frac{\partial\overline{p}}{\partial\overline{\phi}}$	Pressure gradient in rotational direction	$J = \frac{E\overline{R}^2\sigma\beta_0^2\overline{w}_0^2}{KR\overline{T}_0^2}$	Joule Heating Parameter
$\overline{Q}$	Heat generation constant		
$\overline{C}_0$	Initial concentration of the reactant species		

$$
\begin{aligned}
&W(4) = \\
&\frac{1}{2}\rho\left(\frac{1}{2}H\lambda+\frac{1}{2}C+\frac{1}{2}\rho H\lambda^2-\frac{1}{2}\rho C\lambda\right)\left(-\frac{1}{2}\delta\lambda-\frac{1}{2}J\lambda^2\right)+\frac{3}{4}\rho^2\left(-\frac{1}{2}\delta\lambda-\frac{1}{2}J\lambda^2\right)^2\left(\frac{1}{2}H\lambda+\frac{1}{2}C+\frac{1}{2}\rho H\lambda^2-\frac{1}{2}\rho C\lambda\right)\\
&+\frac{1}{2r^2}\left(\frac{1}{2}H\lambda+\frac{1}{2}C+\frac{1}{2}\rho H\lambda^2-\frac{1}{2}\rho C\lambda\right)-\frac{1}{4r}\Lambda\left(\frac{1}{2}H\lambda+\frac{1}{2}C+\frac{1}{2}\rho H\lambda^2-\frac{1}{2}\rho C\lambda\right)^3\\
&-\frac{1}{4r}\rho\Lambda\Bigg[\ \frac{-8}{27r^3}\left(-\frac{1}{2}\delta\lambda-\frac{1}{2}J\lambda^2\right)\left(\frac{1}{2}H\lambda+\frac{1}{2}C+\frac{1}{2}\rho H\lambda^2-\frac{1}{2}\rho C\lambda\right)^3+\frac{4}{9r^2}\left(-\frac{1}{2}\delta\lambda-\frac{1}{2}J\lambda^2\right)\\
&\qquad\left(\frac{1}{2}H\lambda+\frac{1}{2}C+\frac{1}{2}\rho H\lambda^2-\frac{1}{2}\rho C\lambda\right)^3\left(-\frac{1}{2}\delta\lambda-\frac{1}{2}J\lambda^2\right)\\
&\qquad\left(\frac{1}{2}H\lambda+\frac{1}{2}C+\frac{1}{2}\rho H\lambda^2-\frac{1}{2}\rho C\lambda\right)^3+\frac{4}{3r}\left(-\frac{1}{2}\delta\lambda-\frac{1}{2}J\lambda^2\right)\left(\frac{1}{2}H\lambda+\frac{1}{2}C+\frac{1}{2}\rho H\lambda^2-\frac{1}{2}\rho C\lambda\right)^3\Bigg]\\
&+\frac{1}{4}H\left(\frac{1}{2}H\lambda+\frac{1}{2}C+\frac{1}{2}\rho H\lambda^2-\frac{1}{2}\rho C\lambda\right)^3+\frac{1}{4}\rho H\left(\lambda\left(-\frac{1}{2}\delta\lambda-\frac{1}{2}J\lambda^2\right)+\left(\frac{1}{2}H\lambda+\frac{1}{2}C+\frac{1}{2}\rho H\lambda^2-\frac{1}{2}\rho C\lambda\right)\lambda\right)\\
&-\frac{1}{4}\rho C\left(-\frac{1}{2}\delta\lambda-\frac{1}{2}J\lambda^2\right)
\end{aligned}
\tag{23}
$$

Using the DTM approach the solution to velocity is $w = W(0) + W(1)r + W(2)r^2 + W(3)r^3 + W(4)r^4$, that is,

$$
\begin{aligned}
w = {} & \lambda + \left(\frac{1}{2}H\lambda + \frac{1}{2}C + \frac{1}{2}\rho H\lambda^2 - \frac{1}{2}\rho C\lambda\right) r^2 + \left[-\frac{2}{3r}\left(\frac{1}{2}H\lambda + \frac{1}{2}C + \frac{1}{2}\rho H\lambda^2 - \frac{1}{2}\rho C\lambda\right)\right] r^3 \\
& + \left[\frac{1}{2}\rho\left(\frac{1}{2}H\lambda + \frac{1}{2}C + \frac{1}{2}\rho H\lambda^2 - \frac{1}{2}\rho C\lambda\right)\left(-\frac{1}{2}\delta\lambda - \frac{1}{2}J\lambda^2\right) + \frac{3}{4}\rho^2\left(-\frac{1}{2}\delta\lambda - \frac{1}{2}J\lambda^2\right)^2\left(\frac{1}{2}H\lambda + \frac{1}{2}C + \frac{1}{2}\rho H\lambda^2 - \frac{1}{2}\rho C\lambda\right)\right. \\
& \quad + \frac{1}{2r^2}\left(\frac{1}{2}H\lambda + \frac{1}{2}C + \frac{1}{2}\rho H\lambda^2 - \frac{1}{2}\rho C\lambda\right) - \frac{1}{4r}\Lambda\left(\frac{1}{2}H\lambda + \frac{1}{2}C + \frac{1}{2}\rho H\lambda^2 - \frac{1}{2}\rho C\lambda\right)^3 \\
& \quad - \frac{1}{4r}\rho\Lambda\left(\frac{-8}{27r^3}\left(-\frac{1}{2}\delta\lambda - \frac{1}{2}J\lambda^2\right)\left(\frac{1}{2}H\lambda + \frac{1}{2}C + \frac{1}{2}\rho H\lambda^2 - \frac{1}{2}\rho C\lambda\right)^3 + \frac{4}{9r^2}\left(-\frac{1}{2}\delta\lambda - \frac{1}{2}J\lambda^2\right)\right. \\
& \qquad \left(\frac{1}{2}H\lambda + \frac{1}{2}C + \frac{1}{2}\rho H\lambda^2 - \frac{1}{2}\rho C\lambda\right)^3 \\
& \qquad + \left(-\frac{1}{2}\delta\lambda - \frac{1}{2}J\lambda^2\right)\left(\frac{1}{2}H\lambda + \frac{1}{2}C + \frac{1}{2}\rho H\lambda^2 - \frac{1}{2}\rho C\lambda\right)^3 \\
& \qquad \left. + \frac{4}{3r}\left(-\frac{1}{2}\delta\lambda - \frac{1}{2}J\lambda^2\right)\left(\frac{1}{2}H\lambda + \frac{1}{2}C + \frac{1}{2}\rho H\lambda^2 - \frac{1}{2}\rho C\lambda\right)^3\right) \\
& \quad + \frac{1}{4}H\left(\frac{1}{2}H\lambda + \frac{1}{2}C + \frac{1}{2}\rho H\lambda^2 - \frac{1}{2}\rho C\lambda\right) + \frac{1}{4}\rho H\left(\lambda\left(-\frac{1}{2}\delta\lambda - \frac{1}{2}J\lambda^2\right) + \left(\frac{1}{2}H\lambda + \frac{1}{2}C + \frac{1}{2}\rho H\lambda^2 - \frac{1}{2}\rho C\lambda\right)\lambda\right) \\
& \quad \left. - \frac{1}{4}\rho C\left(-\frac{1}{2}\delta\lambda - \frac{1}{2}J\lambda^2\right)\right] r^4
\end{aligned} \tag{24}
$$

To obtain λ, we substitute the boundary condition $W(1) = 0$ into (24), the point $r = 1$, and solve.

Likewise, the scheme (22) is implemented with the Maple software, solutions to temperature for $k = 0, 1, 2$ are:

$$\theta(0) = \lambda$$

$$\theta(1) = 0$$

$$\theta(2) = -\frac{1}{2}\delta\lambda - \frac{1}{2}J\lambda^2$$

$$\theta(3) = -\frac{2}{3r}\left(-\frac{1}{2}\delta\lambda - \frac{1}{2}J\lambda^2\right)$$

$$
\begin{aligned}
\theta(4) = {} & \\
& \frac{1}{2r^2}\left(-\frac{1}{2}\delta\lambda - \frac{1}{2}J\lambda^2\right) - \Gamma\left(\frac{1}{2}H\lambda + \frac{1}{2}C + \frac{1}{2}\rho H\lambda^2 - \frac{1}{2}\rho C\lambda\right)^2 + \frac{2}{3}\rho\Gamma\left(-\frac{1}{2}\delta\lambda - \frac{1}{2}J\lambda^2\right)\left(\frac{1}{2}H\lambda + \frac{1}{2}C + \frac{1}{2}\rho H\lambda^2 - \frac{1}{2}\rho C\lambda\right)^2 \\
& - \frac{1}{4}\Lambda\Gamma\left(\frac{1}{2}H\lambda + \frac{1}{2}C + \frac{1}{2}\rho H\lambda^2 - \frac{1}{2}\rho C\lambda\right)^4 - \frac{1}{4}\delta\left(-\frac{1}{2}\delta\lambda - \frac{1}{2}J\lambda^2\right) - \frac{1}{2}J\lambda\left(\frac{1}{2}H\lambda + \frac{1}{2}C + \frac{1}{2}\rho H\lambda^2 - \frac{1}{2}\rho C\lambda\right)
\end{aligned} \tag{25}
$$

Using the DTM approach the solution to temperature is $\theta = \theta(0) + \theta(1)r + \theta(2)r^2 + \theta(3)r^3 + \theta(4)r^4$, that is,

$$
\begin{aligned}
\theta = {} & \lambda + \left(-\frac{1}{2}\delta\lambda - \frac{1}{2}J\lambda^2\right) r^2 + \left[-\frac{2}{3r}\left(-\frac{1}{2}\delta\lambda - \frac{1}{2}J\lambda^2\right)\right] r^3 \\
& \left[\frac{1}{2r^2}\left(-\frac{1}{2}\delta\lambda - \frac{1}{2}J\lambda\right) - \Gamma\left(\frac{1}{2}H\lambda + \frac{1}{2}C + \frac{1}{2}\rho H\lambda^2 - \frac{1}{2}\rho C\lambda\right)^2 + \frac{2}{3}\rho\Gamma\left(-\frac{1}{2}\delta\lambda - \frac{1}{2}J\lambda^2\right)\left(\frac{1}{2}H\lambda + \frac{1}{2}C + \frac{1}{2}\rho H\lambda^2 - \frac{1}{2}\rho C\lambda\right)^2\right. \\
& \quad \left. - \frac{1}{4}\Lambda\Gamma\left(\frac{1}{2}H\lambda + \frac{1}{2}C + \frac{1}{2}\rho H\lambda^2 - \frac{1}{2}\rho C\lambda\right)^4 + \frac{1}{4}\delta\left(-\frac{1}{2}\delta\lambda - \frac{1}{2}J\lambda^2\right) - \frac{1}{2}J\lambda\left(\frac{1}{2}H\lambda + \frac{1}{2}C + \frac{1}{2}\rho H\lambda^2 - \frac{1}{2}\rho C\lambda\right)\right] r^4
\end{aligned} \tag{26}
$$

To obtain λ, we substitute the boundary condition $\theta(1) = 0$ into (26), the point where $r = 1$, and solve.

Table 3: Distinction between $\theta_{max}(DTM)$ and $\theta_{max}(ADM)$ for C with $\Gamma = \delta = \rho = 1$

$\lvert C\rvert$		$\Lambda = 1$	
	Present Result $\theta_{max}(DTM)$	Iyoko et al. [25] $\theta_{max}(ADM)$	Absolute Difference
0.25	0.02154	0.01057	1.097×10^{-2}
0.5	0.08013	0.04400	3.613×10^{-2}
0.75	0.16029	0.10500	5.53×10^{-2}
1	0.24521	0.20000	4.52×10^{-2}
2	0.50258	1.04000	5.37×10^{-1}

Table 4: Distinction between $\theta_{max}(DTM)$ and $\theta_{max}(ADM)$ for Λ with $\Gamma = \delta = \rho = 1$

Λ		$C = -1$	
	Present Result $\theta_{max}(DTM)$	Iyoko et al. [25] $\theta_{max}(ADM)$	Absolute Difference
0	0.24037	0.14286	9.75×10^{-2}
0.5	0.24282	0.17143	7.14×10^{-2}
1	0.24527	0.20000	4.53×10^{-2}
1.1	0.24568	0.20571	3.99×10^{-2}
1.5	0.24754	0.22857	1.89×10^{-2}

Table 5: Distinction between $\theta_{max}(DTM)$ and $\theta_{max}(ADM)$ for Γ with $\Lambda = -C = \rho = 1$

Γ		$\delta = 1$	
	Present Result $\theta_{max}(DTM)$	Iyoko et al. [25] $\theta_{max}(ADM)$	Absolute Difference
0	0.0	0.0	0.0
1	0.24282	0.20000	4.28×10^{-2}
3	0.44343	0.46667	2.32×10^{-2}
5	0.53658	0.63636	9.98×10^{-2}
6	0.56805	0.70000	1.32×10^{-1}

Table 6: Distinction between $\theta_{max}(DTM)$ and $\theta_{max}(ADM)$ for δ with $\Gamma = -C = \rho = 1$

δ		$\Gamma = 1$	
	Present Result $\theta_{max}(DTM)$	Iyoko et al. [25] $\theta_{max}(ADM)$	Absolute Difference
-0.4	0.15158	0.09091	6.07×10^{-2}
-0.2	0.16372	0.09859	6.51×10^{-2}
0	0.17665	0.10769	6.90×10^{-2}
0.5	0.21130	0.14000	7.13×10^{-2}
1	0.24521	0.20000	4.52×10^{-2}

Table 7: Distinction between $\theta_{max}(DTM)$ and $\theta_{max}(ADM)$ for ρ with $-C = \Lambda = \Gamma = 1$

ρ		$\delta = 1$	
	Present Result $\theta_{max}(DTM)$	Iyoko et al. [25] $\theta_{max}(ADM)$	Absolute Difference
-6	0.31395	$-$	$-$
-4	0.43504	0.70000	2.65×10^{-1}
0	0.37500	0.23333	1.42×10^{-1}
5	0.10732	0.12727	2.00×10^{-2}
6	0.09467	0.11666	2.20×10^{-2}

3. Results and discussion

3.1. Difference between the DTM and ADM

Comparing the solutions from the DTM and ADM, the temperature distribution at the middle of the pipe $\theta(0) = \theta_{max}$ for DTM solution and Adomian decomposition method solution (ADM) of [25] are tabulated when $H = J = 0$. How the two methods vary in terms of their absolute difference is calculated as well.

The behaviour of the temperature at mid-point of pipe when $|C|$ varies from 0.25 to 2.00 is presented in Table 2. The values gotten through DTM approach are realistically larger than the ones from Adomian decomposition method, with the difference increasing from 10^{-2} to 10^{-1} as $|C| > 1$. In Table 3, the non-Newtonian parameter (Λ) is varied and it is observed that the maximum temperature remain very close; even as Λ increases from 0.00 to 1.50. The value of $\theta_{max}(DTM)$ is greater than those of $\theta_{max}(ADM)$, with the difference between the two methods being at most 10^{-2}. The viscous heating parameter Γ is varied in Table 4, where we see that the disparity in the values from DTM and ADM increase from 10^{-2} to 10^{-1} as $\Gamma > 5$. Here, the maximum temperature from the ADM is a bit higher than that of the DTM. In Table 5 we considered the variation of heat generation/absorption parameter δ. The difference between DTM and ADM being 10^{-2} as δ increases from -0.40 to 1.00. Also, the values of the DTM solution are higher than that of the ADM solution. Table 6 shows the difference between the two solutions as values of ρ is increased from -6.00 to 6.00. Whereas, there was no defined value for the temperature when $\rho = -6$ while using the ADM method; a definite value was gotten when the DTM method was used. The $\theta_{max}(DTM)$ reduced steadily for $-4 \leq \rho \leq 6$, but the reduction in $\theta_{max}(ADM)$ was sharp.

3.2. Profiles of Velocity and Temperature

When we input different values for each parameter into equations (24) and (26), the solution for velocity and temperature are represented through graphs. Here, the x-axis is the pipe radius. Figs. 2 – 8 represent the behaviour of the velocity whereas Figs. 9 – 15 depict the behaviour of the temperature.

How the pressure gradient parameter C affects velocity of the fluid is displayed in Fig. 2. As can be seen, the fluid's velocity is zero at pipe's wall for each value of C and then it rises until it becomes maximum at the midpoint. Afterwards, it falls rapidly to zero at the opposite wall of the pipe. As C decreases to -1 from -0.5, fluid velocity at midpoint of pipe increases (this means that as fluid continues to flow, lesser pressure is required to sustain the flow). For the adomian decomposition solution, however, a small fall in C (from -0.5 to -0.75) reduced the velocity. It only increased when $C = -1$.

Fig. 3 is the behavior of velocity as Non-Newtonian material parameter Λ varies. As Λ increases, fluid velocity also rises, although their difference is very small and it seems to remain constant. This is the general influence on velocity caused by increasing Non-Newtonian material parameter. But, the adomian decomposition solution depicted a fall in velocity as Λ increases. The case of a Newtonian fluid ($\Lambda = 0$) has the lesser velocity of fluid flow. This agrees with the fact that no matter how fast Newtonian fluids flow, their viscosity remains constant.

When the viscous heating parameter Γ is varied, the flows velocity profile is shown in Fig. 4. We see that as values of Γ rises, there tend to be a decrement in velocity at pipe's mid-point. This tend to be better than the velocity profile for the ADM, where there was

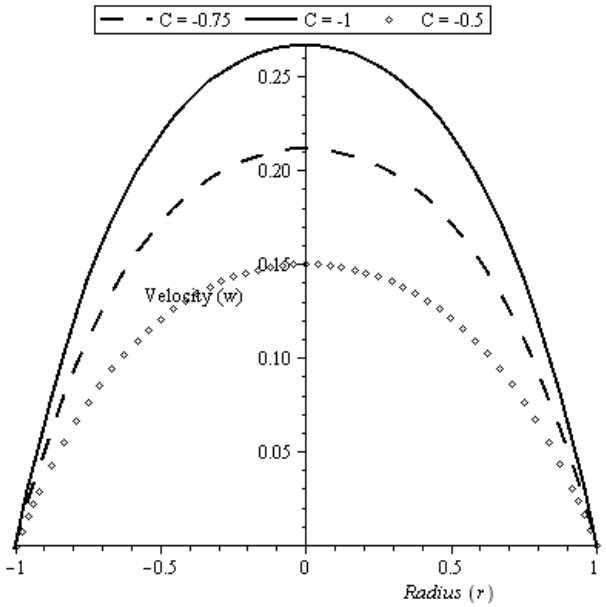

Figure 2: Pressure gradient parameter C versus velocity when $\Lambda = J = H = \rho = \delta = \Gamma = 1$.

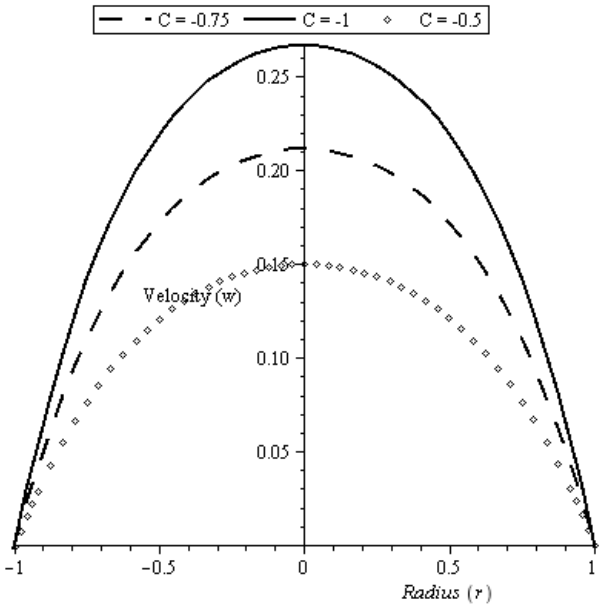

Figure 4: Viscous heating parameter Γ versus velocity when $-C = J = H = \rho = \delta = \Lambda = 1$.

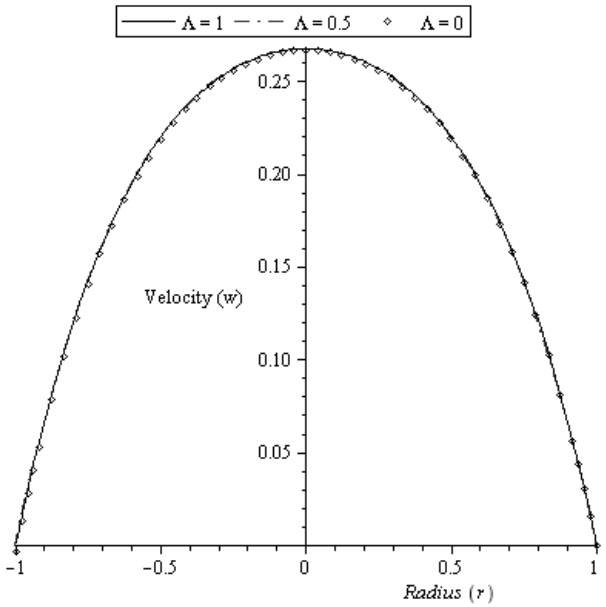

Figure 3: Non-Newtonian material parameter of the fluid Λ versus velocity when $-C = J = H = \rho = \delta = \Gamma = 1$.

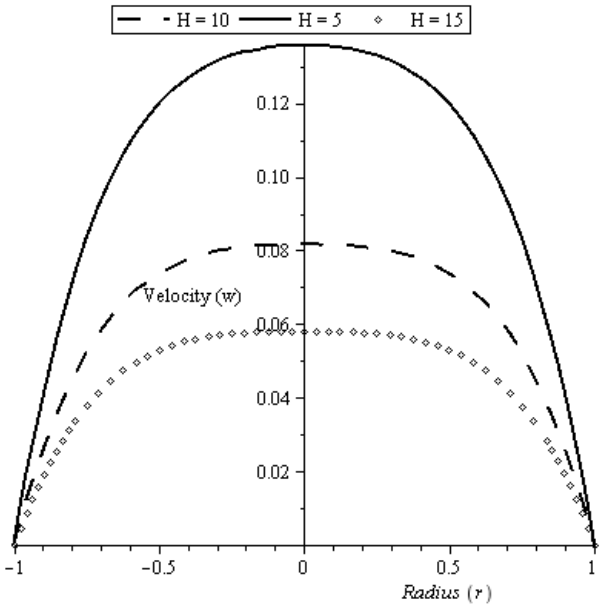

Figure 5: Magnetic effect parameter H versus velocity when $-C = J = \Gamma = \rho = \delta = \Lambda = 1$.

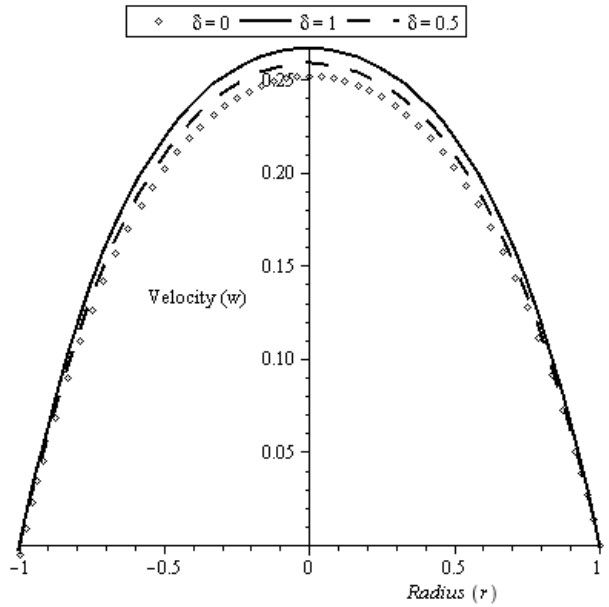

Figure 6: Heat generation parameter δ versus velocity when $-C = J = \Gamma = \rho = H = \Lambda = 1$.

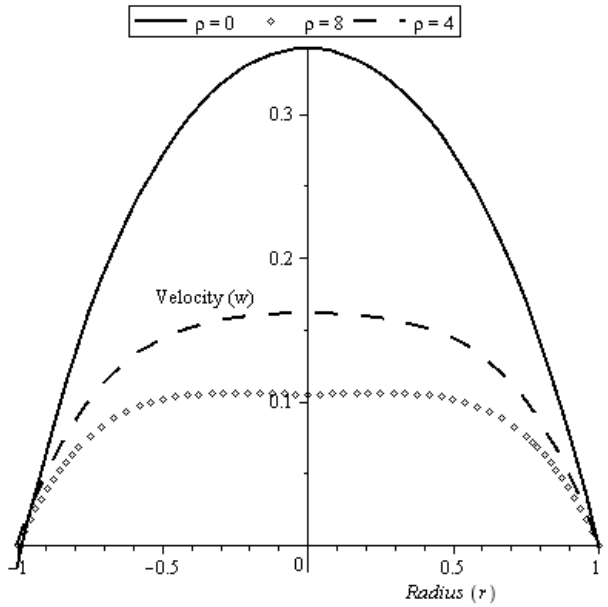

Figure 8: Reynolds' viscosity variational parameter ρ versus velocity when $-C = \delta = \Gamma = J = H = \Lambda = 1$.

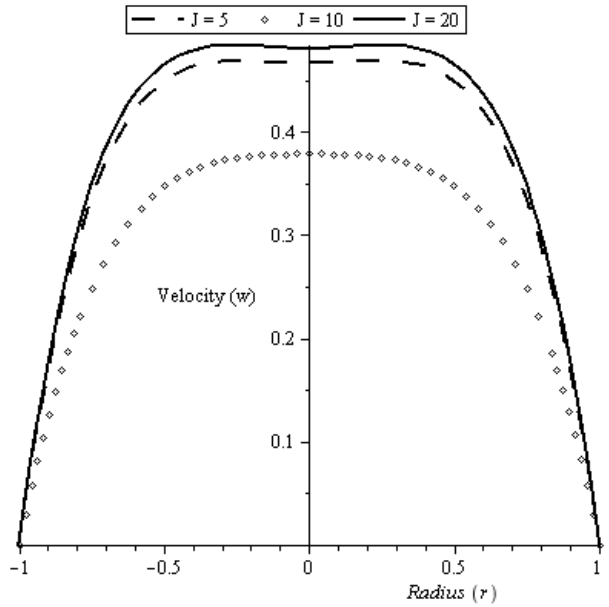

Figure 7: Joule heating parameter J versus velocity when $-C = \delta = \Gamma = \rho = H = \Lambda = 1$.

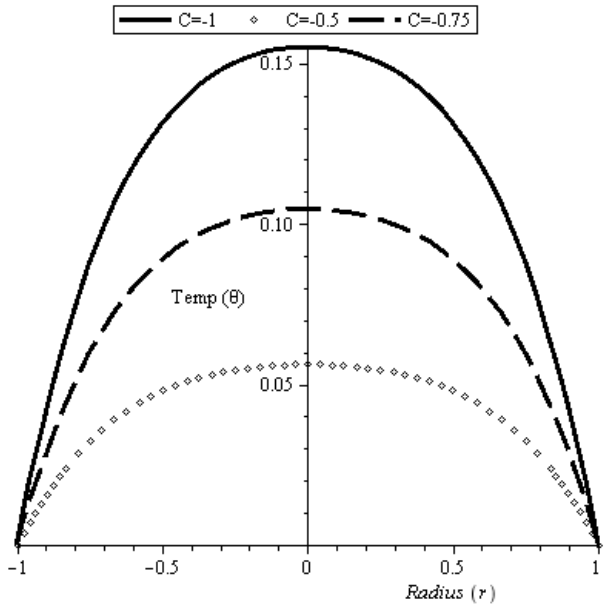

Figure 9: Pressure gradient parameter C versus temperature when $\Lambda = J = H = \rho = \delta = \Gamma = 1$.

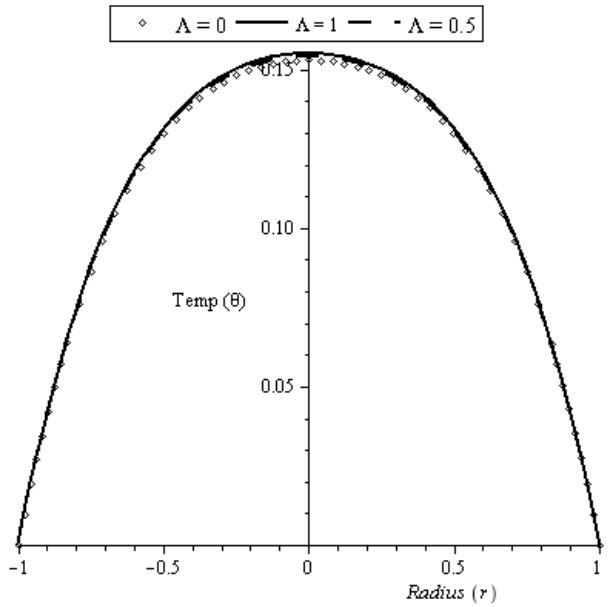

Figure 10: Non-Newtonian material parameter Λ versus temperature when $-C = J = H = \rho = \delta = \Gamma = 1$.

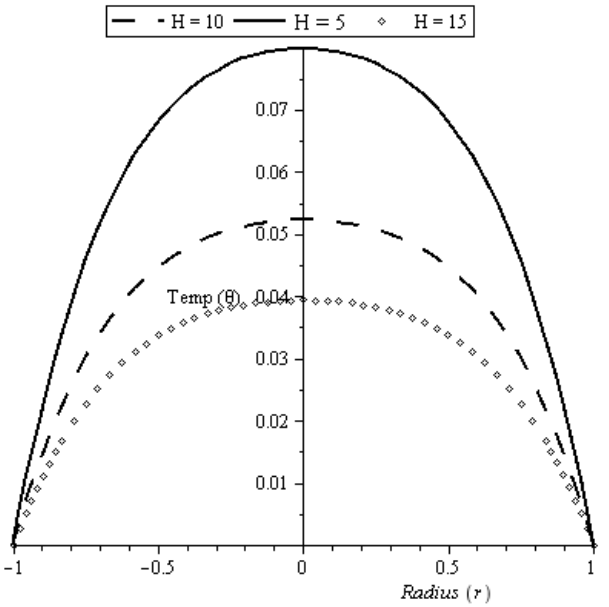

Figure 12: Magnetic effect parameter H versus temperature when $-C = J = \Gamma = \rho = \delta = \Lambda = 1$.

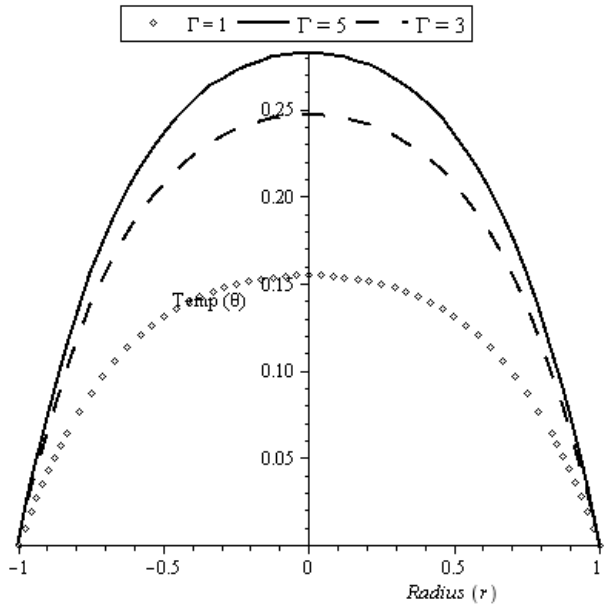

Figure 11: Viscous heating parameter Γ versus temperature when $-C = J = H = \rho = \delta = \Lambda = 1$.

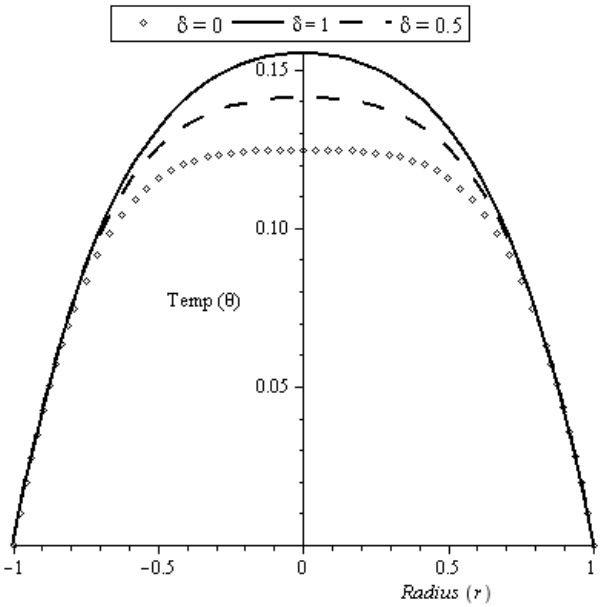

Figure 13: Heat generation parameter δ versus temperature when $-C = J = \Gamma = \rho = H = \Lambda = 1$.

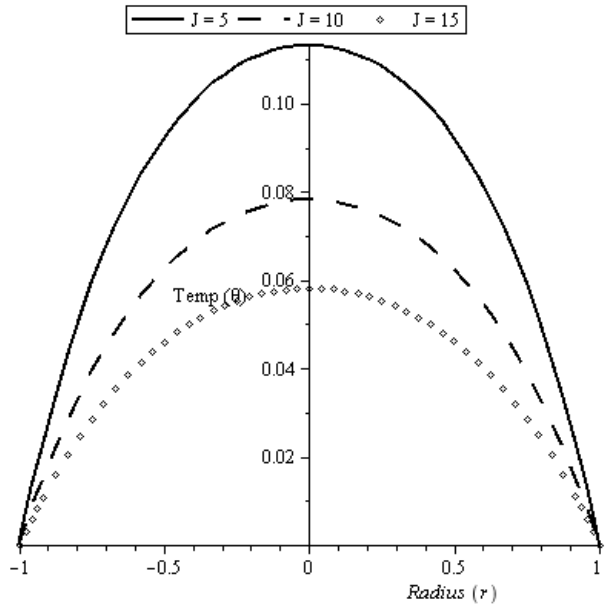

Figure 14: Joule heating parameter J versus temperature when $-C = \delta = \Gamma = \rho = H = \Lambda = 1$.

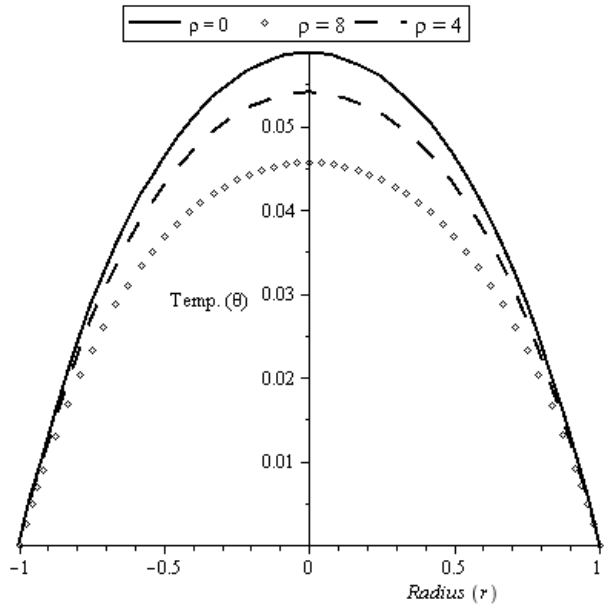

Figure 15: Reynolds' viscosity variational parameter ρ versus temperature when $-C = \delta = \Gamma = J = H = \Lambda = 1$.

a fluctuation in velocity of the fluid when $\Gamma = 5$ (increasing above the value for $\Gamma = 3$ before reducing at the midpoint).

In Fig. 5 the behaviour of fluid velocity as influenced by the magnetic effect parameter H is presented. For every H value, the velocity tends to increase rapidly only in a thin layer near the pipe's wall. Thereafter, it seems constant for a larger part towards the center of the pipe. Increasing H causes fluid velocity to decelerate; this agrees with the fact that a magnetic field makes non-Newtonian fluids become semi-solids. The graphs for the DTM approach looks more refined as compared with those from the ADM-which depicted negative values for velocity at some values of H .

As heat generation parameter δ varies, the behaviour of velocity is shown in Fig. 6. Here, increasing δ brings about an increment in velocity. As δ increases from 0.00 to 1.00, the maximum velocity increases accordingly. Unlike the case of the ADM where there is a fall in the value of the velocity before it later increased.

When the parameter responsible for joule heating J is varied, Fig. 7 demonstrates their corresponding influence on velocity. From it we see maximum velocity happening in-between the pipe's mid-point and the pipe wall. Afterwards, it fell in value before getting to the mid-point of pipe. Increasing J from 5 to 10, the velocity decreases, but further increase in J caused velocity to increase at the pipe's mid-point.

Fig. 8 depicts the influence of Reynolds' viscosity variational parameter ρ on velocity of flow. Clearly, as there is an increment in ρ, we see the pipe's mid-point velocity deceasing. The difference in value of velocity between $\rho = 0$ and $\rho = 4$ is quite large compared to that between $\rho = 4$ and $\rho = 8$. Here also, the DTM approach gives a better progression in velocity with increase in ρ than what ADM gives.

Fig. 9 presents to us the behaviour of the fluid temperature as pressure gradient parameter C is varied. It reveals that a more negative C, results in an increment in the temperature at the pipe's mid-plane. There is a regular difference of 0.05 in the maximum temperature as C moves from $C = -0.5$ to $C = -1$; unlike the case of the ADM solution, where there is a very sharp difference in maximum velocity with varying C .

In the graph depicting how Non-Newtonian material parameter Λ influences fluid's temperature, that is, Fig. 10; increase in Λ causes temperature at mid-point of the pipe to increase. This is what is generally accepted as the influence of Λ on temperature of non-Newtonian fluids. But, the ADM solution gives a reduction in temperature with increase in Λ.

Fig. 11 represents the influence of the viscous heating parameter Γ, and it shows that the fluid temperature increases as Γ increases. The viscous heating parameter Γ acts as a source of heat, it therefore, generally increases fluid temperature.

When the magnetic effect parameter H rises there is reduction in the fluid's maximum temperature (Fig. 12). Although, physically increasing the magnetic parameter corresponds to increase in the resistive force, which in turn increases temperature. The result here becomes interesting, and could be because of the presence of joule heating or heat generation.

The heat generation parameters' effect on behaviour of fluid temperature is depicted in Fig. 13. As heat generation parameters (δ) increases, temperature seems to increase at midpoint of pipe. There is increase in temperature along the wall, which then reaches a maximum at the pipe's center for each δ value.

From the influence of the joule heating parameter (J) represented in Fig. 14, increment in J brings about a fall in the fluid's maximum temperature. Explanation for this behaviour could be because heat generation already exists.

The final parameter to consider is the Reynolds' viscosity variational parameter ρ. Its effect on fluid temperature is shown in Fig. 15, which reveals that the pipe's mid-point temperature reduces

as ρ becomes larger. When the viscosity of the fluid is constant ($\rho = 0$) the temperature records its highest value.

4. Conclusion

Here the model equations of an MHD flow of a third grade fluid was solved by applying the DTM approach. Mapple (13) was used to get an analytic polynomial result to fluid's velocity as well as temperature. Each of the parameters arising in the flow was varied and the behaviour of the fluid's velocity and also temperature was shown graphically. Conclusions are thus:

1. DTM solution converges faster than the Adomian decomposition method (ADM) solution.
2. The magnetic effect parameter brings about reduction of the fluid's velocity and temperature.
3. Very high joule heating parameter increases fluid's velocity while its increase reduces the fluid temperature.
4. Both velocity and temperature experience an increase for negative values of the pressure gradient parameter.
5. Decline of the fluid's velocity as well as temperature occurs with increment of non-Newtonian material parameter.
6. There is a decrease in velocity for increased viscous dissipation parameter, and it, on the other hand, increases temperature.

Conflicts of interests

No conflicts of interests were declared by the authors.

References

[1] Zhou J K, Differential Transformation and Its Applications for Electrical Circuits, Huarjung University Press, Wuuhahn, China, (1986).

[2] Jang M J, Chen C L & Liu Y C, Two-dimensional differential transform for partial differential equations, *Appl. Math. Comput.*, 121 (2001) 261-270.

[3] Momania S, & Suat Ertürk V, Solutions of non-linear oscillators by the modified differential transform method, *Computers and Mathematics with Applications*, 55 (2008) 833-842.

[4] Abdel-Halim Hassan I H, On solving some eigenvalue-problems by using a differential transformation, *Appl. Math. Comput.*, 127 (2002) 1-22.

[5] Joneidi A A, Ganji D D & Babaelahi M, Differential transformation method to determine fin efficiency of convective straight fins with temperature dependent thermal conductivity, *International Communications in Heat and Mass Transfer*, 36 (2009) 757-762.

[6] Abazari R, & Borhanifar A, Numerical study of the solution of the burgers and coupled burgers equations by a differential transformation method, *Computers and Mathematics with Applications*, 59 (2010) 2711-2722.

[7] Oke A S, Convergence of differential transform method for ordinary differential equations, *Journal of Advances in Mathematics and Computer Science*, 24 (2017) 6: 1-17.

[8] Domairry G, Sheikholeslami M & Ashorynejad H R, The application of differential transformation method to solve nonlinear differential equation governing jeffery-hamel flow with high magnetic field, *International Journal of Nonlinear Dynamics in Engineering and Sciences*, 3 (2011) 1: 111–122.

[9] Soltanalizadeh B, Application of differential transformation method for solving a fourth-order parabolic partial differential equation, *International Journal of Pure and Applied Mathematics*, 78 (2012) 3: 299-308.

[10] Gbadeyan J A, Idowu A S, Okedayo G T, Ahmed L O & Lawal O W, Effect of suction on thin film flow of a third grade fluid in a porous medium down an inclined plane with heat transfer, *International Journal of Scientific and Engineering Research*, 5 (2014) 4: 748-754.

[11] Costa S, De T, & Sandberg D, Mathematical model of a smoldering log, *Combustion and Flame*, 139 (2004) 227-238.

[12] Makinde O D, Hermite-Pade approach to thermal radiation effect on inherent irreversibility in a variable viscosity channel flow, *Computers and Mathematics with Applications*, 58 (2009) 2330-2338.

[13] Okoya S S, Disappearance of criticality for reactive third grade fluid with reynold's model viscosity in a flat channel, *International Journal of Non-linear Mechanics*, 46 (2011) 9: 1110-1121.

[14] Bansal L, Magnetofluiddynamics of Viscous Fluids, Jaipur Publishing House, Jaipur, India, OCLC 70267818, (1994).

[15] Cha J E, Ahn Y C & Moo-Hwan Kim, Flow measurement with an electromagnetic flowmeter in two-phase bubbly and slug flow regimes, *Flow Measurement and Instrumentation*, 12 (2002) 5-6: 329-339.

[16] Tendler M, Confinement and related transport in extrap geometry, *Nuclear Instruments and Methods in Physics Research*, 207 (1983) 1-2: 233-240.

[17] Mossino J, Some nonlinear problems involving a free boundary in plasma physics, *Journal of Differential Equations*, 34 (1979) 1: 114-138.

[18] Nijsing R, & Eifler W, A computational analysis of transient heat transfer in fuel rod bundles with single phase liquid metal cooling, *Nuclear Engineering and Design*, 62 (1980) 1-3: 39-68.

[19] Branover H & Gershon P, MHD Turbulence Study. Report BGUN-RDA-100-176. Ben-Gurion University, (1976).

[20] [20] Holroyd R J, An experimental study of the effect of wall conductivity, non-uniform magnetic field and variable-area ducts on liquid metal flow at high hartmann number, part 1: ducts with non-conducting wall, *Journal of Fluid Mechanics*, 93 (1979) 609-630.

[21] Smith P, Some asymtoticextremum principle for magnetohydrodynamic pipe flow, *Applied Science Resources*, 24 (1971) 452-466.

[22] Aiyesimi Y M, Okedayo G T & Lawal O W, MHD flow of a third grade fluid with heat transfer and slip boundary condition down an inclined plane, *Mathematical Theory and Modeling*, 2 (2012) 9: 108-120,.

[23] [23] Aiyesimi Y M, Abah S O & Okedayo G T, Radiative effects on the unsteady double diffusive MHD boundary layer flow over a stretching vertical plate, *American Journal of Scientific Research*, 65 (2012) 51-61.

[24] Jayeoba O J & Okoya S S, Approximate analytical solutions for pipe flow of a third grade fluid with variable models of viscosities and heat generation/absorption, *Journal of Nigerian Mathematical Society*, 31 (2012) 207-227.

[25] Iyoko M O, Okedayo G T, Aboiyar T & Ikpakyegh L N, MHD flow of a third grade fluid in a cylindrical pipe in the presence of Reynolds' model viscosity and joule heating, *FUW Trends in Science and Technology Journal*, 2 (2017) 1B: 514-520.

[26] Massoudi M & Christe I, Effect of variable viscosity and viscous dissipation on the flow of third grade fluid in a pipe, *International Journal of Non-linear Mechanics*, 30 (1995) 5: 687-699.

[27] Yurusoy M & Pakdemirli M, Approximate analytical solution for the flow of a third grade fluid in a pipe, *International Journal of Non-linear Mechanics*, 37 (2002) 2: 187-195.

[28] Olajuwon B I, Flow and natural convection heat transfer in a power law fluid past a vertical plate with heat generation, *International Journal of Non-linear Science*, 7 (2009) 1: 50-56.

[29] Pakdemirli M & Yilbas B S, Entropy generation for pipe flow of a third grade fluid with vogel model viscosity, *International Journal of Non-linear Mechanics*, 41 (2006) 3: 432-437.